Table DR5: *Kinetic and Diffusion-Domain Data, and Inversion-Model Parameters for K-Feldspar Samples EUT-2 and EUT-35*

```
SAMPLE INFO:   LU1433 EUT2 Kspar
(Best fit is   2.51, worst fit is   3.09)

          CRS ITERATIONS:  4000
   MODEL DURATION (m.y.):    200.0
              TIME NODES:    15
CONSTRAINING BRACKETS tT:     4
   TIME    TMIN   TMAX
  200.0   450.0   500.0
  190.0     0.0   500.0
   20.0     0.0   500.0
    0.0     0.0   500.0
MAX MONTE-CARLO HEATING RATE:   5.0   MAX MONTE-CARLO COOLING RATE:  50.0
        MAX CRS HEATING RATE:   5.0           MAX CRS COOLING RATE: 200.0
    CRS AMPLIFICATION FACTOR:   1.30
      SUBSET SIZE, POOL SIZE:   15   150
           FITTING CRITERION:   1.00
              FITTING OPTION:   1  (mean percent)
          DIFFUSION GEOMETRY:   2  (infinite-slab)
              RESTART OPTION:   0  (new start from Monte-Carlo histories)
DISCRETIZATION DELTA-TEMPERATURE:   5.0
           LOVERA SERIES CUT-OFF:   1.0e-04
      FLAG TO WRITE FULL REPORTS:   1

DOMAIN INFO
-----------
Domains:  8
      E        D0        frac.   Tc (10˚C/m.y.)
 1  39.14  1.30950e+20  0.016       135
 2  39.14  4.32617e+18  0.019       164
 3  39.14  8.37730e+15  0.025       231
 4  39.14  3.27419e+15  0.110       243
 5  39.14  2.09461e+15  0.070       248
 6  39.14  1.06931e+15  0.050       257
 7  39.14  8.18661e+14  0.110       261
 8  39.14  1.08169e+14  0.600       290

Goal Age Spectrum
-----------------
Goal spectrum steps:  58
      f39     age    error  skip?
  1  0.001    57.0   10.0   0
  2  0.001    85.8    7.3   1
  3  0.003   102.5    3.7   1
  4  0.004   105.0    2.4   1
  5  0.007   120.6    1.5   1
  6  0.009   114.1    1.6   1
  7  0.012   124.0    1.6   1
  8  0.015   119.8    1.3   1
  9  0.019   128.1    1.1   1
 10  0.022   128.4    1.3   1
 11  0.027   132.3    1.2   1
 12  0.029   131.4    1.2   1
 13  0.033   132.2    1.4   1
 14  0.036   134.9    1.0   1
 15  0.039   136.7    1.0   1
```

16	0.041	138.1	1.1	1
17	0.044	135.6	1.0	1
18	0.046	138.3	0.9	1
19	0.049	137.6	1.1	1
20	0.051	137.7	1.1	1
21	0.054	134.9	1.5	1
22	0.055	136.2	1.3	1
23	0.059	134.2	0.9	1
24	0.065	133.7	1.0	1
25	0.072	132.3	0.9	1
26	0.082	133.2	1.3	1
27	0.093	132.0	0.8	1
28	0.108	129.8	1.0	1
29	0.129	128.7	1.0	1
30	0.155	128.8	0.5	1
31	0.182	129.9	0.7	1
32	0.255	129.7	0.8	1
33	0.291	131.1	0.6	1
34	0.371	132.8	0.7	1
35	0.377	132.4	0.7	1
36	0.396	133.0	0.7	1
37	0.451	132.9	0.9	1
38	0.456	133.1	0.6	1
39	0.470	133.1	1.0	1
40	0.500	133.9	0.5	1
41	0.520	135.2	0.8	1
42	0.538	135.4	0.9	1
43	0.552	134.7	1.0	1
44	0.555	137.3	1.0	1
45	0.564	133.1	1.0	1
46	0.596	134.3	0.6	1
47	0.658	135.0	1.4	0
48	0.736	137.3	0.7	0
49	0.850	140.1	0.8	0
50	0.919	142.4	0.5	0
51	0.935	140.7	0.9	0
52	0.955	137.2	0.9	0
53	0.977	139.8	0.7	0
54	0.996	143.9	0.8	0
55	0.999	142.0	1.2	0
56	1.000	144.1	6.6	0
57	1.000	138.3	20.9	0
58	1.000	141.8	25.4	0

Heating Schedule Actually Used

Heating Steps: 58

	Temp. (C)	Time
1	426.3	10.0
2	438.1	10.0
3	468.1	10.0
4	492.7	10.0
5	529.9	10.0
6	522.1	10.0
7	561.5	10.0
8	557.1	10.0
9	598.7	10.0
10	601.3	10.0
11	664.8	10.0
12	661.1	10.0

13	688.9	10.0
14	677.2	10.0
15	699.1	10.0
16	684.5	10.0
17	723.9	10.0
18	713.7	10.0
19	753.1	10.0
20	742.9	10.0
21	780.9	10.0
22	763.3	10.0
23	813.0	10.0
24	848.0	10.0
25	878.7	10.0
26	918.1	10.0
27	944.4	10.0
28	986.7	10.0
29	1030.5	10.0
30	1071.4	10.0
31	1099.1	10.0
32	1237.8	10.0
33	1194.0	10.0
34	1331.3	10.0
35	1072.9	10.0
36	1201.3	10.0
37	1356.1	10.0
38	1107.9	10.0
39	1224.7	10.0
40	1329.8	10.0
41	1306.4	10.0
42	1300.6	10.0
43	1288.9	10.0
44	1131.2	10.0
45	1248.0	10.0
46	1434.9	10.0
47	1586.8	10.0
48	1703.6	10.0
49	1890.4	10.0
50	1913.8	10.0
51	1691.9	10.0
52	1785.3	10.0
53	1925.5	10.0
54	2205.8	10.0
55	2252.5	10.0
56	1505.0	10.0
57	1505.0	10.0
58	1505.0	10.0

===

SAMPLE INFO: LU1341 EUT35 Kspar
(Best fit is 3.68, worst fit is 3.23)

CRS ITERATIONS: 4000
MODEL DURATION (m.y.): 200.0
TIME NODES: 15
CONSTRAINING BRACKETS tT: 4

TIME	TMIN	TMAX
200.0	450.0	500.0
190.0	0.0	500.0
20.0	0.0	500.0
0.0	0.0	500.0

```
MAX MONTE-CARLO HEATING RATE:   5.0   MAX MONTE-CARLO COOLING RATE:   5.0
        MAX CRS HEATING RATE:   0.0           MAX CRS COOLING RATE: 500.0
    CRS AMPLIFICATION FACTOR:   1.40
      SUBSET SIZE, POOL SIZE:   15   150
           FITTING CRITERION:   1.00
              FITTING OPTION:   1  (mean percent)
          DIFFUSION GEOMETRY:   2  (infinite-slab)
              RESTART OPTION:   0  (new start from Monte-Carlo histories)
DISCRETIZATION DELTA-TEMPERATURE:   5.0
           LOVERA SERIES CUT-OFF:   1.0e-04
      FLAG TO WRITE FULL REPORTS:   1
```

DOMAIN INFO

Domains: 9

	E	D0	frac.	Tc (10˚C/m.y.)
1	44.80	9.10131e+21	0.010	156
2	44.80	6.01318e+20	0.020	179
3	44.80	1.84121e+19	0.025	211
4	44.80	1.50350e+18	0.025	237
5	44.80	6.36948e+16	0.050	275
6	44.80	2.67365e+16	0.150	286
7	44.80	1.88410e+16	0.050	291
8	44.80	1.74222e+16	0.020	292
9	44.80	9.75223e+14	0.650	334

Goal Age Spectrum

Goal spectrum steps: 58

	f39	age	error	skip?
1	0.001	48.4	11.2	0
2	0.002	60.2	6.0	1
3	0.003	71.0	1.8	1
4	0.005	77.7	0.8	1
5	0.009	83.9	0.7	1
6	0.011	86.4	0.3	1
7	0.015	93.5	0.6	1
8	0.018	100.2	0.4	1
9	0.022	107.0	1.4	1
10	0.025	112.8	0.8	1
11	0.030	120.0	1.3	1
12	0.033	120.8	0.4	1
13	0.037	123.6	0.5	1
14	0.040	125.2	1.0	1
15	0.043	126.3	0.7	1
16	0.046	128.0	0.5	1
17	0.049	126.3	0.4	1
18	0.052	129.8	0.6	1
19	0.057	129.6	0.7	1
20	0.060	129.1	0.7	1
21	0.066	129.3	0.5	1
22	0.069	130.1	0.5	1
23	0.076	129.3	0.4	1
24	0.085	130.5	0.4	1
25	0.100	128.7	0.5	1
26	0.117	128.5	0.8	1
27	0.133	128.9	0.5	1
28	0.150	126.2	0.7	1
29	0.166	127.2	0.8	1
30	0.185	126.8	0.6	1

31	0.206	127.1	0.7	1
32	0.256	127.7	0.3	1
33	0.293	127.2	0.6	1
34	0.359	127.3	0.5	1
35	0.365	128.3	0.5	1
36	0.383	127.0	0.4	1
37	0.420	126.8	0.5	1
38	0.423	127.1	0.6	1
39	0.433	128.1	0.5	1
40	0.461	128.4	0.6	1
41	0.483	128.3	0.4	1
42	0.501	127.7	0.7	1
43	0.518	127.5	0.7	1
44	0.520	124.0	0.9	1
45	0.526	124.2	0.4	1
46	0.533	127.0	0.7	1
47	0.547	126.2	0.8	1
48	0.569	126.3	0.6	0
49	0.615	124.5	0.3	0
50	0.730	123.8	0.5	0
51	0.869	124.3	0.3	0
52	0.932	125.9	0.3	0
53	0.960	126.9	0.5	0
54	0.992	128.4	0.5	0
55	0.999	127.7	0.6	0
56	1.000	126.1	1.8	0
57	1.000	130.6	9.6	0
58	1.000	131.3	40.5	0

Heating Schedule Actually Used

Heating Steps: 58

	Temp. (C)	Time
1	442.1	10.0
2	455.1	10.0
3	471.9	10.0
4	502.6	10.0
5	536.7	10.0
6	531.9	10.0
7	562.4	10.0
8	568.1	10.0
9	602.4	10.0
10	604.6	10.0
11	637.1	10.0
12	627.6	10.0
13	654.6	10.0
14	662.6	10.0
15	687.4	10.0
16	690.3	10.0
17	716.6	10.0
18	707.9	10.0
19	745.8	10.0
20	734.1	10.0
21	766.3	10.0
22	753.1	10.0
23	802.8	10.0
24	843.6	10.0
25	902.8	10.0
26	937.1	10.0
27	960.4	10.0

28	988.2	10.0
29	1010.1	10.0
30	1036.4	10.0
31	1059.7	10.0
32	1154.6	10.0
33	1156.1	10.0
34	1243.7	10.0
35	1049.5	10.0
36	1151.7	10.0
37	1239.3	10.0
38	1061.2	10.0
39	1131.2	10.0
40	1253.9	10.0
41	1256.8	10.0
42	1259.7	10.0
43	1259.7	10.0
44	1107.9	10.0
45	1178.0	10.0
46	1201.3	10.0
47	1271.4	10.0
48	1341.5	10.0
49	1458.3	10.0
50	1639.3	10.0
51	1767.8	10.0
52	1750.3	10.0
53	1715.2	10.0
54	1925.5	10.0
55	2252.5	10.0
56	1505.0	10.0
57	1505.0	10.0
58	1505.0	10.0

3D thermo-mechanical numerical models

Three-dimensional, coupled thermal-mechanical numerical models were constructed to study orogen scale kinematics and dynamics during the evolution of the St. Elias Orogen, southern Alaska (Hooks, 2009; Koons and others, 2010). These models allow for the testing of the influence of boundary, surface, and geometric characteristics on the evolution of plate corner within a continuum mechanics framework. The model geometry encompasses an area of dimensions 890 km (north-south= Y) by 640 km (east-west =X) with a thickness of 20 km (=Z) (fig. DR2). An isotropic conductive-advective thermal model (thermal conductivity (k) = 2.6 $Wm^{-1}C^{-1}$; radiogenic volumetric heat source (A_v) = 0.37 μWm^{-3}) and Mohr-Coulomb (~upper 15 km; ϕ = 30; cohesion = 44 MPa) and thermally-defined plastic yield condition (~lower 5 km; yield strength = 100 MPa) mechanical models are used to define the thermal and mechanical constitutive models. The models include no initial weaknesses; faults and shear zones develop as the model evolves as a function of partitioning and focusing of strain.

The initial velocity conditions are imposed on the base of the model over an area corresponding to the spatial extent of the Yakutat terrane (south of the Chugach-St. Elias Fault and west of the Fairweather Fault) consistent with its observed motions (~50 mm/yr; Fletcher and others, 2008). All margins of the model, except the surface, have fixed velocity conditions. The top and bottom (-20 km) of the model are conditioned with fixed temperatures of 0 and 400 °C, respectively (fig. DR2).

The modeling path first develops a reference Tectonic Model in the absence of topography or erosion; then the natural topography (Topographic Model*)* and an erosion scheme (Erosion Model*)* are successively applied as initial boundary conditions. The present topography, including bathymetry, was derived from a global 1-minute DEM sampled at the model discretization (~10 km spacing; Smith and Sandwell, 1997). The presence of anomalous topography has been shown to alter the stress state of the crust and can lead to feedback between uplift and localization of strain (Koons and others, 2002). To emphasize the influence of erosion, vigorous erosional conditions are applied based upon the spatial extent of current glaciations and are based on the assumption that glacial erosion maintains a near constant elevation during exhumation (Hallet and others, 1996; Meigs and Sauber, 2000). The erosion model employed for this study maintains the model nodes at a constant elevation (fixed between 500 and 1000 m) within the defined zone of erosion during the model run. Material passing through the model surface at these zones is essentially removed from the model system.

Hooks (2009) shows that the resultant deformation patterns produced by the model are relatively insensitive to the initial surface boundary conditions (i.e. erosion and topography). This suggests that the strain patterns observed within the orogen are primarily controlled by the kinematics and tectonic geometry. As the models reproduce the uplift and strain patterns observed within southern Alaska (Hooks, 2009; Koons et al., 2010), it is assumed that the model kinematic conditions are aptly characterized.

Backward projections of particle paths are extracted from the model. This technique assumes that the velocity conditions have reached near steady-state conditions and define the flux of material through the orogen (Hooks, 2009). Three particle paths were extracted from three locations of exhumation (A, B, and C on Figure 7). Temperatures and velocity conditions were extrapolated from the model grid to yield the three-dimensional paths extrapolated to the depth reach near constant values. Times were calculated using the velocities along the paths.

Supplemental Model Figure

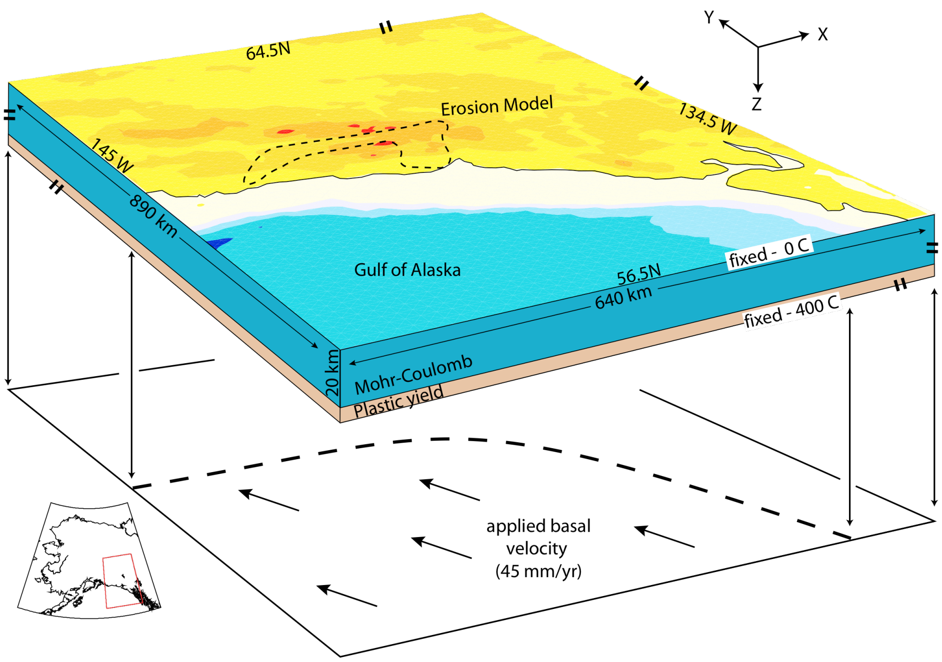

Figure DR2: Model diagram showing 3D geometry and boundary conditions for the numerical model (modified from Hooks, 2009). Not all model boundaries have fixed velocity conditions, except the model surface, which is free to deform. The model surface is conditioned with natural topography (color fill; 1000m contours) and an erosion model (see the dashed outline) that maintains a constant topography by removing material from the surface. A basal drag is applied to the model over the area of the Yakutat Terrane (see drop down plane) by giving the area the observed velocity of the Yakutat Terrane (~45 mm/yr). The model surface and base (~20 km depth) are given fixed temperatures of 0 C and 400 C, respectively.

REFERENCES

Cundall, P. A., and Board, M., 1988, A microcomputer program for modeling large-strain plasticity problems, in Swododa, C., editor, Numerical Methods in Geomechanics, Proceedings 6th International Conference on Numerical Methods in Geomechanics, Innsbruck, Austria, April 11–15: Rotterdam, Balkema, p. 2101–2108.

Hallet, B., Hunter, L., and Bogen, J., 1996, Rates of erosion and sediment evacuation by glaciers; a review of field data and their implications: Global and Planetary Change, v. 12, p. 213-235.

Harrison, T.M., Grove, M., Lovera, O.M., and Zeitler, P.K., 2005. Continuous thermal histories from inversion of closure profiles, in Low-Temperature Thermochronology: Techniques, Interpretations, and Applications, Reviews in Mineralogy & Geochemistry, v. 58, edited by P.W. Reiners PW and T.A. Ehlers. pp. 389-409, Mineralogical Society of America, Chantilly, VA.

Hooks, B.P., 2009, Geodynamics of terrane accretion within southern Alaska, Unpublished Doctoral Dissertation, University of Maine, Orono, ME, 188 p.

Meigs, A. and Sauber, J. 2000, Southern Alaska as an example of the long-term consequences of mountain building under the influence of glaciers. *in* Stewart, I. et al., editors, Glacio-seismotectonics; ice sheets, crustal deformation and seismicity:. Quaternary Science Reviews v. 19, p. 1543-1562.

Koons, P.O., Hooks, B.P., Upton, P., Barker, A.D., and Pavlis, T.L., 2010, Three-dimensional mechanics of Yakutat convergence in the southern Alaskan plate corner: Tectonics, in press.

Smith, W. H. F., and Sandwell, D. T., 1997, Global seafloor topography from satellite altimetry and ship depth soundings: Science, v. 277, p. 1957-1962.

Zeitler, P.K. (2004) Arvert 4.0.1. Inversion of $^{40}Ar/^{39}Ar$ age spectra. User's Manual (http://www.ees.lehigh.edu/EESdocs/geochron/downloads/arvert401guide-US.pdf).